Journal of Physiology (1991), **435**, *pp.* 303–331
With 8 figures
Printed in Great Britain

KINETIC PROPERTIES OF THE GLYCINE RECEPTOR MAIN- AND SUB-CONDUCTANCE STATES OF MOUSE SPINAL CORD NEURONES IN CULTURE

BY ROY E. TWYMAN* AND ROBERT L. MACDONALD*†

*From the Departments of *Neurology and †Physiology, University of Michigan Medical Center, Ann Arbor, MI 48104, USA*

(*Received 4 April 1990*)

SUMMARY

1. The kinetic properties of the two most frequent conductance states of glycine receptor channels from somata of mouse spinal cord neurones in cell culture were investigated using the outside-out patch clamp technique. At low concentrations of glycine (0·5, 1 and 2 μM), single-channel currents were recorded with two predominant amplitudes corresponding to a dominant or main-conductance state of about 42 pS and a sub-conductance state of about 27 pS. Both conductance states opened singly and in bursts of several openings. Total current evoked and single-channel opening frequency increased as glycine concentration was increased from 0·5 to 2 μM.

2. For both conductance states mean open times were increased and open time frequency histograms were shifted to longer times as glycine concentration was increased from 0·5 to 2 μM. For both conductance states, three exponential components were required to fit best open time frequency distribution histograms at all glycine concentrations (0·5, 1 and 2 μM). The time constants of the exponential components for each conductance state were not significantly different across concentration, suggesting that the main- and sub-conductance states of the channel each opened into at least three open states. For the main-conductance state, the time constants were $1{\cdot}09 \pm 0{\cdot}09$, $4{\cdot}06 \pm 0{\cdot}26$ and $9{\cdot}79 \pm 0{\cdot}30$ ms. For the sub-conductance state, the time constants were $0{\cdot}55 \pm 0{\cdot}04$, $2{\cdot}64 \pm 0{\cdot}35$ and $8{\cdot}57 \pm 1{\cdot}08$ ms. The increase in long open times with concentration was due primarily to a shift in relative frequency of occurrence of openings from the shortest to the two longest open states.

3. Closed time frequency distributions of closures between main-conductance state openings, closures between sub-conductance state openings and closures between both main- and sub-conductance state openings were fitted with multiple exponential components, suggesting that the channel had several closed states. The two shortest time constants ($0{\cdot}16 \pm 0{\cdot}01$ and $1{\cdot}26 \pm 0{\cdot}13$ ms) did not vary significantly with concentration (0·5–2 μM) or method of analysis. The longer time constant varied with concentration.

4. Bursts were defined as groups of openings surrounded by closures greater than a critical closed time. For both conductances states, mean burst durations were increased and burst duration frequency histograms were shifted to longer times as glycine concentration was increased from 0·5 to 2 μM. Burst duration frequency

MS 8406

histograms contained four exponential components for the main-conductance state and three exponential components for the sub-conductance state. Across concentration, the number of exponential components that were fitted was independent of the number of bursts in the histograms. The time constants did not vary significantly with concentration and were $0{\cdot}78 \pm 0{\cdot}11$, $2{\cdot}50 \pm 0{\cdot}27$, $9{\cdot}14 \pm 1{\cdot}17$ and $28{\cdot}2 \pm 5{\cdot}5$ ms for the main-conductance state and were $0{\cdot}58 \pm 0{\cdot}14$, $4{\cdot}11 \pm 0{\cdot}31$ and $22{\cdot}9 \pm 3{\cdot}9$ ms for the sub-conductance state. For both conductance states, the increase in burst duration with concentration was due to a relative shift from shorter duration bursts to longer duration bursts.

5. From these data we conclude that glycine gates its receptor channel open to two predominant conductance states whose open and burst properties are qualitatively similar suggesting a similar general mechanism for activation or gating of both conductance states. Brief openings and brief bursts of each conductance state appear to have been evoked primarily from singly liganded receptors, while longer duration openings and bursts appear to have been evoked primarily from fully liganded receptors. However, the two conductance states differed in opening and closing rates suggesting that (a) the receptor subunit composition or configurations were different for each conductance state or (b) there exists different protein domains on a single receptor/channel which regulate gating of each conductance state. Kinetic schemes for the gating of the main- and sub-conductance states are discussed.

INTRODUCTION

The amino acid glycine, a major inhibitory neurotransmitter in the mammalian central nervous system, binds to glycine receptors to open chloride ion channels (Aprison & Werman, 1965; Werman, Davidoff & Aprison, 1967; Curtis, Hosli, Johnston & Johnston, 1968; Curtis, Hosli & Johnston, 1968; Young & Snyder, 1974*a*, *b*; Barker & Ransom, 1978; Barker & McBurney, 1979; Gold & Martin, 1983; Betz & Becker, 1988). The glycine receptor is composed of a large glycoprotein containing at least three polypeptide subunits (α, β and γ) of unknown stoichiometry (Pfeiffer, Graham & Betz, 1982; Becker, Hermans-Gorgmeyer, Schmitt & Betz, 1986). It has been suggested that the receptor forms a pentamer of $\alpha_3\beta_2$ and has a membrane-anchoring subunit γ (Langosch, Leo & Betz, 1988). The 48 kDa stychnine-binding α-subunit of the receptor has been shown to have substantial amino acid sequence similarity to the α-subunit of the nicotinic acetylcholine (nACh) receptor and to the α- and β-subunits of the γ-aminobutyric acid$_A$ (GABA) receptor (Schofield, Darlison, Fujita, Burt, Stephenson, Rodriguez, Rhee, Ramachandran, Reale, Glencorse, Seeburg & Barnard, 1987; Greeningloh, Rienitz, Schmitt, Methfessel, Zensen, Bereuther, Gundelfinger & Betz, 1987; Schmieden, Grenningloh, Schofield & Betz, 1989).

Like other ligand-gated receptors such as nACh, GABA and glutamate receptors, glycine evokes complex currents with multiple unitary current amplitudes (Cull-Candy, Miledi & Parker, 1981; Dionne & Liebowitz, 1982; Hamill, Bormann & Sakmann, 1983; Sakmann, Hamill & Bormann, 1983). Single-channel current-recording techniques have shown that glycine receptor currents contain at least four different current amplitudes corresponding to channel conductances of about 44, 30, 19 and 12 pS (Hamill, Marty, Neher, Sakmann & Sigworth, 1981; Hamill *et al.* 1983;

Bormann, Hamill & Sakmann, 1987; Smith, Zorec & McBurney, 1989). In mouse spinal neurones, a 44 pS conductance state was the most frequent or main-conductance state, and the next frequent was a 30 pS sub-conductance state (Bormann *et al.* 1987).

Although ligand-gated receptor channels might share similar properties, the kinetic mechanisms that underlie coupling of glycine receptor binding to ion channel opening and closing (gating) are unclear. In addition, the relationships between glycine receptor activation and the gating kinetics of channels with multiple conductance states have not been reported. Even though the conductance properties are different, it is possible that the mechanisms regulating the gating of each conductance state are similar. Since different conductance states can be resolved using single-channel patch clamp techniques, the kinetic properties of gating of different conductance states are amenable to analysis. We, therefore, have recorded single-channel currents from outside-out patches of mouse spinal cord neurones grown in cell culture to investigate the gating kinetic properties of the main- and sub-conductance states of glycine receptor channels. To study the gating kinetics, low concentrations of glycine (0·5, 1 and 2 μM) were used to activate and to minimize desensitization of the glycine receptor channel (Akaike & Kaneda, 1989).

METHODS

Cell culture

To obtain spinal cord neurone cultures, timed pregnant mice were anaesthetized using CO_2 narcosis and then their necks were fractured. The 12- to 14-day-old fetuses were removed and decapitated. The spinal cords were dissected from the fetuses and were mechanically dissociated to yield a single-cell suspension and grown in culture medium as described previously (Macdonald, Rogers & Twyman, 1989). Cultures were maintained for 2–5 weeks prior to being used in these experiments.

Solutions

Thirty minutes prior to the first recording, the medium used to grow and maintain the cultures was exchanged for 2 ml of extracellular solution which consisted of the following (in mM): 142 NaCl, 8·1 KCl, 1 $CaCl_2$, 6 $MgCl_2$, 10 glucose, 10 HEPES (pH ~ 7·4). The solution used in the micropipettes contained (in mM): 153 KCl, 1 $MgCl_2$, 10 HEPES, 5 EGTA (pH ~ 7·4). This combination of extracellular and micropipette solutions resulted in a chloride equilibrium potential (E_{Cl}) of about 0 mV and a potassium equilibrium potential (E_K) of about −75 mV. All recordings were performed at room temperature (20–23 °C).

Glycine and drug application

A 1 mM-glycine (Sigma) stock solution in distilled water was prepared prior to experiments and frozen in 1 ml aliquots. The stock solution of glycine was diluted with extracellular solution to final concentrations of 0·5, 1 or 2 μM on the day of each experiment. Strychnine (Sigma) was dissolved in external bathing solution at a concentration of 100 nM on the day of the experiment. Bicuculline (Sigma) was dissolved in dimethyl sulphoxide to a concentration of 10 mM. Serial dilutions in external bathing solution were made to a final concentration of 10 μM and used within 2 h of preparation. Glycine (0·5, 1 or 2 μM), a mixture of glycine (1 μM) and strychnine (100 nM) or a mixture of glycine (1 μM) and bicuculline (19 μM) was applied to patches for at least 20 s by pressure ejection from micropipettes similar to that previously described (Macdonald *et al.* 1989). Micropipettes were moved to within 10 μm of patches only during the time of each application.

Current recording

Recording micropipettes were constructed as described previously (Macdonald *et al.* 1989). Recordings were obtained using a model L/M EPC-7 amplifier (List Medical Instruments, Darmstadt). Single-channel currents were low-pass filtered (3 dB at 10 kHz, eight-pole Bessel filter,

Frequency Devices, Haverhill, MA, USA) and simultaneously recorded on a video-cassette recording (VCR) system (Sony SL-2700) via a digital audio processor (Sony PCM-501ES, modified to 0–20 kHz, 14-bit/44 kHz sampling frequency) and on a chart recorder (Gould Inc.) using a low-pass (3 dB at 2 kHz), eight-pole Bessel filter interposed.

Single-channel current analysis

For the present study, data were accepted for analysis if only rare multiple openings (no evidence of three or more simultaneous openings) were detected during the application of glycine. If possible, all concentrations of glycine were applied to each patch prior to rupture of the patch or loss of channel activity.

For analysis, single-channel data were played back from the VCR system and digitized (20 kHz (50 μs/sample point), 14 bit, 40·96 points/pA, Tecmar A/D converter) for computer (80386 based processors) analysis with a low-pass (3 db at 2 kHz), eight-pole Bessel filter interposed. Single-channel data were analysed by computer using locally written analysis programs. Channel amplitude distributions were determined prior to temporal analysis of channel current (Colquhoun & Sigworth, 1983; Macdonald *et al.* 1989). To obtain an accurate estimate of channel amplitude (Colquhoun & Sigworth, 1983), openings were constrained to be greater than twice the rise time of the low-pass filter (rise time = 170 μs, determined empirically). Channel openings to three independent mean current amplitudes and their respective closings were reliably measured using the 50% threshold crossing method for each mean current amplitude (Colquhoun & Sigworth, 1983). Data were analysed simultaneously for the three channel amplitudes in consecutive 50–100 ms segments. Channel detection was initiated by current deviation from baseline greater than 50% of the mean amplitude of each channel. To be accepted as a valid opening, the mean current following detection had to be within a specified window (approximately 1·5–2 standard deviations of the noise variance) above and below one of the three mean channel amplitudes. Channel closing was detected by crossing 50% of the continuous mean channel amplitude of that opening.

Durations of detected closings and openings less than twice the system dead time (dead time = 70 μs) were counted as unresolved open and closed times, respectively. Detected openings with a duration greater than twice the system dead time but less than twice the system rise time (sampled points at 150, 200, 250, 300 and 350 μs) were compensated for amplitude distortion due to the limited system response. The magnitude of amplitude compensation was determined empirically. Constant-amplitude pulses of 150–350 μs durations were measured at the system output to determine the amplitude compensation factor for each duration (about 1·4 for 150 μs and 1·03 for 350 μs). Such compensation would have little effect on open duration time constants and relative proportions of the exponential components since open duration histograms were fitted starting from bins that were greater than twice the system rise time. The number of openings detected at each amplitude level was affected by the compensation and those openings with short time constants were primarily affected. For example, if all of the openings had a time constant of about 0·5 ms, the compensation could affect about 33% of the number of detected openings. In practice, we have found that the compensation usually affects 5–20% of the briefest openings. The actual number of detected openings affected was dependent on the relative proportion of short openings to long openings in the open duration distributions.

In this study, openings with amplitudes smaller than the amplitude of sub-conductance state openings were counted as closures while multiple and ambiguous openings were rejected (deleted). After detection, the output contained condensed data consisting of a series of open and closed durations and their amplitudes. The data then could be analysed selectively for main- or sub-conductance state openings or a combination of conductance states.

The open and closed times reported in this study are observed times. Due to the presence of missed or unresolved events, the observed event times are greater than the true times (Colquhoun & Sigworth, 1983). For example, correction of mean open time for missed openings can be obtained by re-estimating the mean open time from the exponential components determined from fits of the open time distributions (open time correction in Table 1). This type of correction, however, does not correct for the effect of missed closures. Accurate correction of both open and closed time distributions cannot be done without a specific model of the gating mechanism, which at present is unavailable (Blatz & Magleby, 1986).

Analysis of closed times presented at least two additional difficulties. Since the data contained

a small number of multiple simultaneous main-conductance state openings and openings to other conductance states, it was difficult to determine unambiguously which closed times represented 'main-conductance state closed times' or 'sub-conductance state closed times'. For the purposes of this study, closed times were analysed using three different assumptions. First, all closed times between all openings (multiple-, main- and sub-conductance states) were analysed. Secondly, it was assumed that closed times between main-conductance state openings were gated independently of other conductances. In this analysis, non-main-conductance state openings were counted as closures while periods containing multiple openings were rejected (deleted). Thirdly, it was assumed that closed times between sub-conductance state openings were gated independently of other conductance states.

Definition of bursts

Bursts might be defined as openings or groups of openings separated by relatively long closed periods (Colquhoun & Sigworth, 1983). For the purpose of this analysis, a critical closed time, t_c, was chosen such that all openings separated by closures less than t_c belonged within a burst, and bursts were separated by closures greater than t_c. Three t_cs were calculated using the method of equal proportions for each of the three closed time definitions (Colquhoun & Sakmann, 1985; Macdonald *et al.* 1989).

Curve fitting and statistics

Frequency histograms were binned to minimize bin promotion errors according to methods previously described (McManus, Blatz & Magleby, 1987; Macdonald *et al.* 1989). Exponential curve fitting to determine the maximum likelihood estimates of time constants and areas (Colquhoun & Sigworth, 1983) was performed using locally written programs described previously (Macdonald *et al.* 1989; Twyman, Rogers & Macdonald, 1990; Stat Library, IMSL, Inc, Houston, TX, USA). Error ranges for the estimates were calculated using maximum likelihood ranges ($m = 2$) which corresponded to about a 95% confidence interval. The number of significant exponential components was determined by fitting with increasing numbers of exponentials until the χ^2 of the estimated fit and the data were within the 95% confidence interval for accepting the null hypothesis (no difference between the estimated fit and data). Distributions of open, closed or burst durations were fitted over the same ranges for each concentration of glycine. Mean data are presented as mean ± S.D. unless otherwise indicated.

RESULTS

Glycine receptor single-channel currents

Prior to glycine application, occasional brief spontaneous currents were recorded (Fig. 1*A*). Following application of glycine, bursting inward chloride currents were evoked in 89% of patches (thirty-two of thirty-six patches). The bursting currents evoked by glycine (1 μM; Fig. 1*B*) were reversibly reduced by the glycine antagonist strychnine (100 nM; Fig. 1*C* and *D*; Young & Snyder, 1974*b*). Bicuculline (10 μM), a $GABA_A$ receptor antagonist (Novak, Young & Macdonald, 1982), had no effect on the single-channel currents evoked by glycine (1 μM; not shown). Responses evoked from a single patch were often reproducible and could be evoked for up to 90 min. Occasionally, after repeated application, current activity decreased significantly or stopped for prolonged periods. Therefore, glycine receptor currents were accepted for analysis only if they were evoked reproducibly prior to patch break-down. All three glycine concentrations were applied to twenty-four of thirty-two patches prior to patch break-down.

At least four conductance levels were apparent, but only two conductance levels were resolved well in the single-channel records (Fig. 2*B*). The larger conductance state (Fig. 2*B*, double asterisks) generally was recorded more frequently and was

open longer than the smaller conductance state (Fig. 2*B*, single asterisk). Consistent with this observation, current amplitude histograms (0·04 pA bin width) contained a distribution of amplitudes that were best fitted with two Gaussian functions (not illustrated). Current amplitudes at −75 mV were 3·18±0·27 pA and 2·06±0·17 pA.

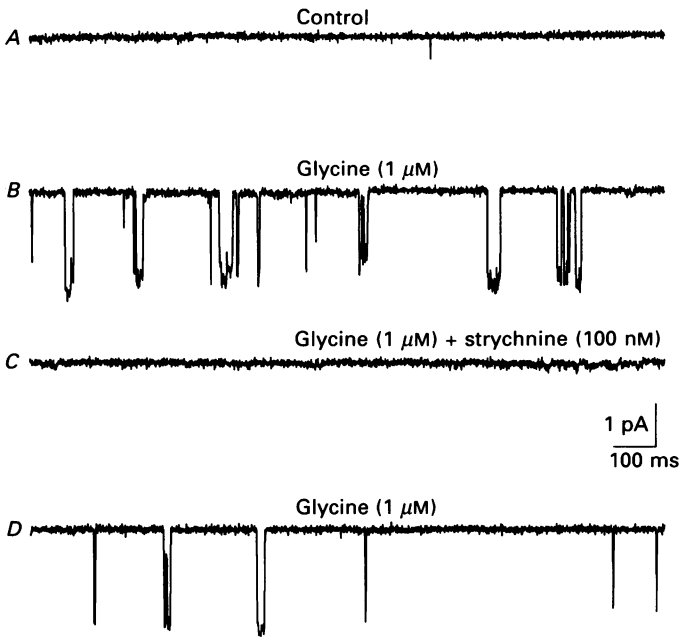

Fig. 1. Glycine (1 μM) evoked single-channel currents in outside-out patches obtained from spinal cord neurones voltage clamped at −75 mV. Solutions were as described in the text. *A*, in the absence of applied glycine, brief spontaneous inward (down-going) unitary currents were recorded. *B*, glycine (1 μM) evoked increased channel openings that were composed predominantly of a 42 pS main-conductance state (double asterisks) and a 27 pS sub-conductance state (single asterisk). *C*, inward currents evoked by glycine (1 μM) were reduced by strychnine (100 nM). *D*, responses returned to control after removal of the antagonist. Time and current calibrations apply throughout.

Single-channel currents reversed at about 0 mV. Channel chord conductances from all patches ($n = 36$) were 42·4±3·5 and 27·5±2·3 pS for the high and low conductance states, respectively. Smaller conductances of about 19 and 12 pS apparent in the raw data traces were poorly resolved due to their small amplitude and low frequency of occurrence. Current amplitudes of the larger or main-conductance state and the smaller or sub-conductance state varied linearly with membrane potential and extrapolated to a reversal potential near 0 mV (E_{Cl}) (not illustrated). In one patch, the current–voltage relationships of the main-conductance and sub-conductance states over the range of −100 to −25 mV were linear and had slope conductances of 44·6 ($r = 0·96$) and 28·7 ($r = 0·97$) pS. At potentials more positive than −25 mV, channel openings were poorly resolved or were contaminated by potassium currents.

For valid openings, opening to the larger conductance level accounted for 70·2±5·8% of the open duration. Openings to the smaller conductance level

accounted for 25·0 ± 6·1 % while openings to an even smaller conductance level of about 19 pS accounted for only 4·8 ± 0·3 %. There was no apparent concentration-dependent shift in the relative proportion of the main- (range 65–76 % of total open duration) and sub-conductance (range 19–31 % of total open duration) levels. The

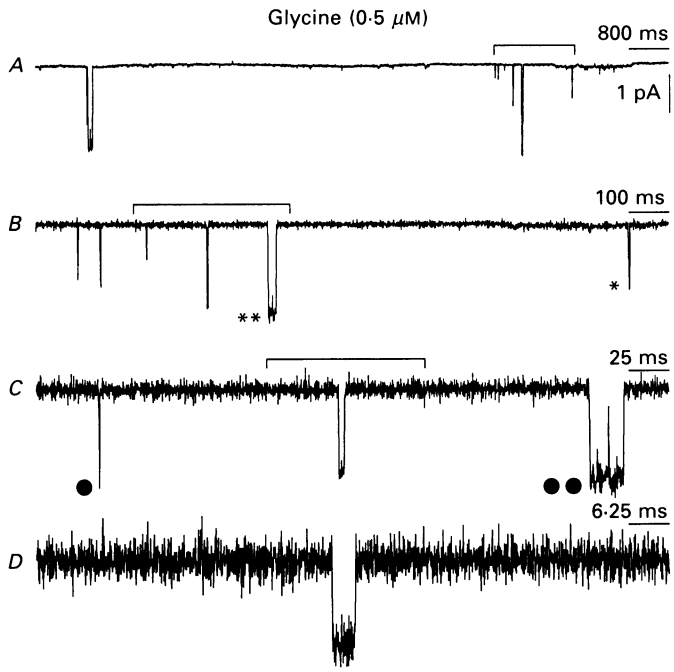

Fig. 2. Glycine (0·5 μM) evoked inward currents that contained single and bursting currents. Currents are shown at increasing time resolution (*A–D*). The portion of current record under the bracketed horizontal line above each trace is presented expanded in time in the tracing below it. The single filled circle indicates a brief, solitary opening and the double filled circles indicate a burst of openings. Openings to the 27 pS sub-conductance state (*B*, single asterisk) might be found intermixed among 42 pS main-conductance state openings (*B*, double asterisks). Time calibration for each trace is shown at right above the trace. Current calibration applies throughout.

percentages of transitions of the main-conductance state to the sub-conductance state (without an observed closing) relative to detected main-conductance state openings were 0·58, 1·16 and 0·64 % for 0·5, 1 and 2 μM-glycine, respectively. The percentages of transitions of the sub-conductance state to the main-conductance state (without an observed closure) relative to detected openings of the sub-conductance state were 2·02, 4·92 and 1·64 % over the same concentration range. Assuming independent 42 and 27 pS channels and unobserved closures with durations less than twice the system dead time, the expected percentages of apparent main-conductance to sub-conductance state transitions were 0·0021, 0·0071 and 0·0250 % over the same glycine concentration range. The expected percentages for apparent sub-conductance to main-conductance state transitions were 0·0010, 0·0034 and 0·0112 %, respectively.

Open properties

Glycine (0·5, 1 and 2 μM) evoked complex currents (Figs 2, 3 and 4) which were often brief and composed of single openings (Fig. 2*C*, single filled circle) or were prolonged and consisted of a burst of sequential openings and closings (Fig. 2*C*,

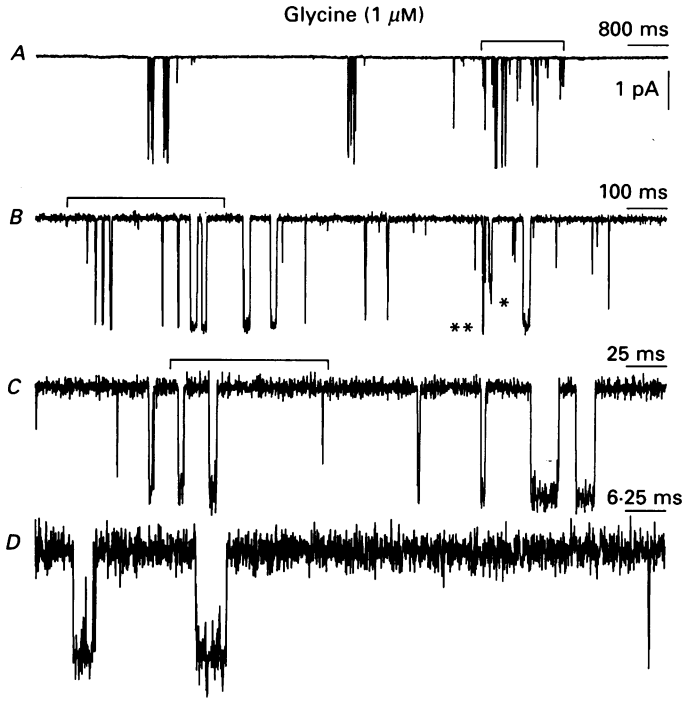

Fig. 3. Glycine (1 μM) evoked inward currents that contained single and bursting currents. The currents were increased in frequency and duration when compared to those evoked by 0·5 μM-glycine (see also Figs 2 and 4). See Fig. 2 legend for details.

double filled circles). With increasing temporal resolution, the pattern of openings was complex and consisted of multiple consecutive openings and closings (Figs 2*A–D*, 3*A–D* and 4*A–D*). At each concentration, openings to the 27 pS sub-conductance state (single asterisk, Figs 2*B*, 3*B* and 4*B*) were intermixed among 42 pS main-conductance state openings (double asterisks, Figs 2*B*, 3*B* and 4*B*).

The currents evoked by glycine varied with concentration (Figs 2, 3 and 4). At −75 mV, prior to the application of glycine, rare, brief spontaneously occurring currents were usually seen (Fig. 1*A*). With increasing concentration (0·5, 1 and 2 μM), glycine evoked an increasing frequency of openings and bursts with increasing complexity (Figs 2, 3 and 4). Average currents (the sum of the mean current amplitude of each of the openings times their duration and divided by the total agonist application duration) for the main-conductance state increased with concentration (0·5–2 μM) from 29 to 105 fA (Table 1). In addition, average currents for the sub-conductance state increased over the same concentration range from 7 to 34 fA. To assess total average glycine receptor current, multiple simultaneous

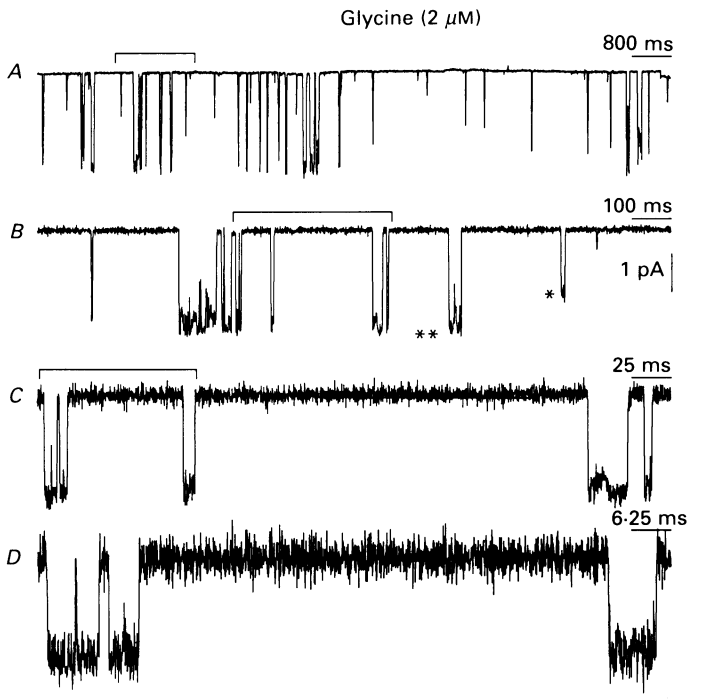

Fig. 4. Glycine (2 μM) evoked inward currents that contained single and bursting currents. The currents were increased in frequency and duration when compared to those evoked by 0·5 and 1 μM-glycine (see also Figs 2 and 3). See Fig. 2 legend for details.

TABLE 1. Glycine receptor main- and sub-conductance states: open and closed properties

	Conductance					
	42 pS			27 pS		
Glycine concentration (μM)	1·5	1·0	2·0	0·5	1·0	2·0
Average current (fA)	29	74	105	7	12	34
Opening frequency (s^{-1})	2·1	4·1	4·9	1·6	2·2	5·2
Mean open time (ms)	4·3	5·7	7·0	2·1	2·7	3·2
Corrected mean open time (ms)	3·9	5·1	5·9	1·6	2·0	3·2
Mean percentage of time open (%)	0·91	2·35	3·41	0·34	0·58	1·64
Mean closed time (ms)	476	244	204	625	455	192
Number of openings	9838	14747	14490	7590	7693	15529
Number of patches	27	30	28	27	30	28

Openings per second, mean open time, mean closed time, percentage open and number of openings were derived from detected 42 pS main-conductance and 27 pS sub-conductance state openings (see Methods). Corrected mean open time was calculated by taking the sum of the relative area of each exponential component in the open time histogram multiplied by the time constant of the component (corrected mean open time = $a_1\tau_1 + a_2\tau_2 + a_3\tau_3$).

openings and openings to other conductance states were not rejected. Total average current evoked by glycine (0·5–2 μM) increased with concentration from 37 to 142 fA.

From 0·5 to 2 μM, the frequency of channel openings increased from 2·1 to 4·9

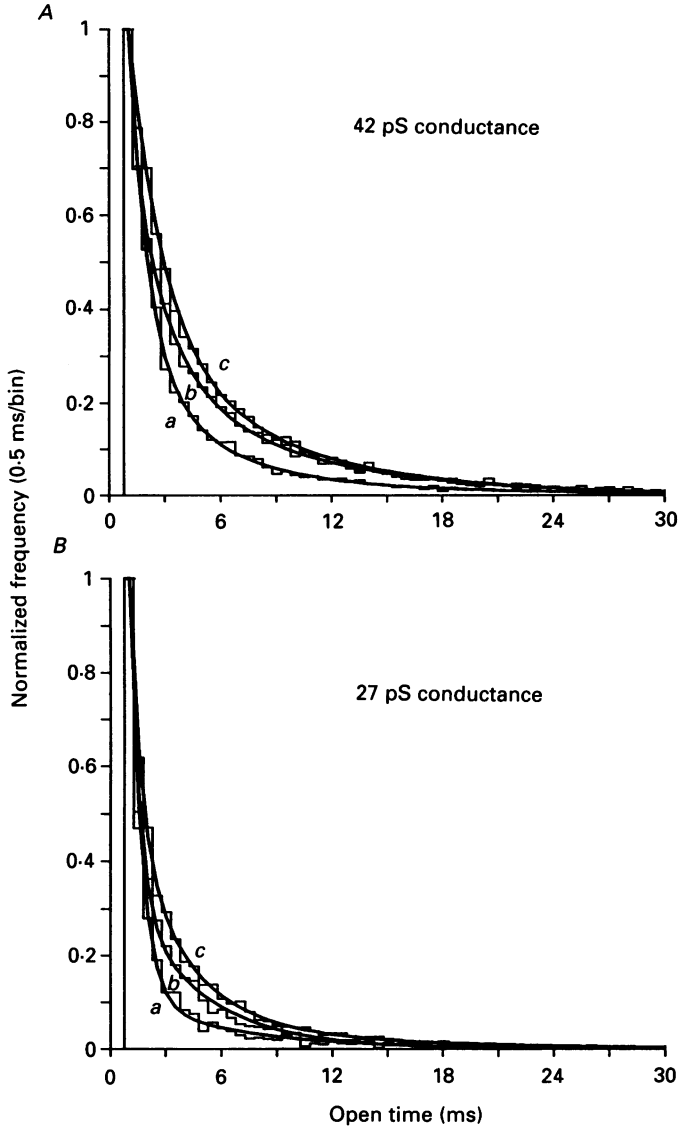

Fig. 5. Open time frequency histograms of the main-conductance (*A*) and sub-conductance (*B*) state openings were fitted with three exponential components. Frequency distributions of the durations of openings evoked by glycine (0·5, 1 and 2 μM) were put into 0·5 ms bins and displayed for clarity over a range of 1–30 ms. Distributions were normalized and overlaid to display relative frequency distribution. Curves were drawn according to the fits (see text). For each conductance state, the lowest curve (*a*) is for 0·5 μM, the middle curve (*b*) is for 1 μM and the highest curve (*c*) is for 2 μM glycine. The numbers of openings in the histograms at each concentration are the same as those provided in Table 1.

openings per second for the main-conductance state and 2·6 to 5·2 openings per second for the sub-conductance state (Table 1). Mean open times of glycine receptor main- and sub-conductance states varied with concentration (0·5–2 μM), increasing

from 4·3 to 7·0 ms and 2·1 to 3·2 ms, respectively (Table 1). When corrected for undetected openings, mean open times of the main- and sub-conductance states increased from 3·9 to 5·9 ms and 1·6 to 3·2 ms, respectively, when glycine concentration was increased. As a result of increased opening frequency and mean open time, the percentage of time the channel was open in the main-conductance state during glycine application increased from 0·91 to 3·41% as glycine concentration increased from 0·5 to 2 μM. Similarly for the sub-conductance state, the percentage of time the channel was open increased from 0·34 to 1·64% as glycine concentration increased. Mean open durations for each conductance state varied little (2·0 ± 3·3%) when the data at each concentration were divided into twelve consecutive 5 s periods and analysed from the beginning of glycine application. This demonstrated stationarity of open states of the channels. However, from the beginning of glycine application, opening frequency and percentage open were decreased 59 ± 4·7 and 67 ± 4·5%, respectively. Opening frequency and the percentage the channel was open stabilized approximately 10–30 s after onset of glycine application. Thus, since open-state properties were unchanged, the decreased current following exposure to glycine was primarily due to decreased channel opening frequency and may have been due to desensitization.

The distributions of open times were fitted best by multiple exponential components

The frequency distributions of open times produced by the application of glycine (0·5–2 μM) were obtained by pooling open times for each conductance state from several patches at each concentration. Results from the analysis of individual patches containing large numbers of openings were not significantly different from pooled data. At each glycine concentration (0·5–2 μM), the open time distributions for the main-conductance state (Fig. 5*A*) had a larger proportion of longer openings than for the sub-conductance state (Fig. 5*B*). As glycine concentration increased, there was a shift in the open time distribution to longer open times for both conductance states.

The open time frequency histograms (0·5–2 μM-glycine) were fitted with multiple exponential components. For the main-conductance state, three exponential components were required to fit best each of the distributions. Exponential components were designated 1 to 3 for the shortest to the longest time constant, respectively. The time constants (τ_i) for each respective component overlapped at each concentration (Table 2). The time constants averaged 1·09 ± 0·09, 4·06 ± 0·26 and 9·79 ± 0·30 ms for components 1, 2 and 3, respectively. The relative area (a_i) for each component was a measure of the relative frequency of occurrence of each component opening (Table 2). The relative area of the open time distribution represented by component 1 decreased from 0·42 to 0·20 as glycine concentration was increased while the proportion due to both components 2 and 3 increased from 0·58 to 0·80.

Similarly for the sub-conductance state, three exponential components were required to fit best each of the distributions (0·5–2 μM-glycine). The exponential components with the shortest to the longest time constants were designated components 1, 2 and 3, respectively. The time constants for each respective component overlapped at each concentration (Table 2). The time constants averaged 0·55 ± 0·04, 2·62 ± 0·35 and 8·57 ± 1·08 ms for components 1, 2 and 3, respectively.

The relative area of the open time distribution represented by component 1 decreased from 0·48 to 0·25 as glycine concentration was increased while the proportion due to both components 2 and 3 increased from 0·52 to 0·75 (Table 2). Thus, the glycine concentration-dependent increase in mean open times for both conductance states was due to a concentration-dependent shift in the relative

TABLE 2. Glycine receptor main- and sub-conductance states: open time constants and relative areas

[Glycine] (μM)	42 pS main-conductance state		
	τ_1	τ_2	τ_3
0·5	1·05 (0·94–1·18)	3·98 (3·48–4·59)	9·84 (8·20–11·3)
1	1·03 (0·89–1·22)	4·35 (4·00–4·73)	9·47 (8·60–10·3)
2	1·19 (0·95–1·50)	3·86 (3·42–4·31)	10·1 (9·14–11·0)
	a_1	a_2	a_3
0·5	0·42 (0·39–0·44)	0·38 (0·35–0·42)	0·20 (0·16–0·24)
2	0·23 (0·19–0·26)	0·48 (0·45–0·50)	0·29 (n.d.–n.d.)
2	0·20 (0·17–0·22)	0·39 (0·36–0·41)	0·41 (0·37–0·44)
[Glycine] (μM)	27 pS sub-conductance state		
	τ_1	τ_2	τ_3
0·5	0·51 (0·47–0·56)	2·23 (2·03–2·45)	8·34 (7·07–9·73)
1	0·53 (0·51–0·55)	2·76 (2·54–3·01)	7·62 (6·46–8·75)
2	0·59 (0·51–0·68)	2·89 (2·69–3·09)	9·74 (7·82–11·3)
	a_1	a_2	a_3
0·5	0·48 (0·46–0·50)	0·40 (0·38–0·43)	0·12 (0·09–0·14)
1	0·34 (0·33–0·35)	0·48 (0·45–0·51)	0·18 (0·14–0·21)
2	0·25 (0·24–0·27)	0·51 (0·49–0·53)	0·24 (0·20–0·26)

Time constants (τ_i) and relative areas (a_i) of exponential components fitted to open time frequency histograms (see Fig. 5 for plots) for the 42 pS main-conductance and 27 pS sub-conductance states evoked by glycine (0·5, 1 and 2 μM). Components 1, 2 and 3 correspond to exponential components with the shortest, intermediate and longest time constants, respectively. Ranges in parentheses were calculated by likelihood intervals ($m = 2$). n.d. are ranges that could not be determined.

frequency of occurrence of the three open time exponential components without significant alteration of their time constants.

Closed properties

Closed times were evaluated using three different assumptions (see Methods). In each, the distribution of closed times ranged from the shortest accurately detected duration of 150 μs to several seconds. The mean closed times between all detected openings to the main- and sub-conductance states decreased from 270 to 99 ms as glycine concentration was increased (0·5–2 μM). The mean closed times between main-conductance state openings decreased from 476 to 204 ms and the mean closed times between sub-conductance state openings decreased from 625 to 192 ms as glycine concentration was increased (Table 1).

For each closed time analysis method, the closed times were widely distributed (microseconds to seconds) and were placed in frequency distributions of 'short' (Fig.

6) and 'long' closed times (Fig. 7). The distribution of short closed times (Fig. 6) ranged from 0·3 to 30·0 ms in bins of 0·1 ms. Long closed times (Fig. 7) ranged from 5 to 1500 ms in bins of 5 ms. The short closed times determined by each method of analysis varied little as a function of concentration (Fig. 6*A*, *B* and *C*). The long closed time histograms showed a shift to shorter closed times as glycine concentration was increased (Fig. 7*A*, *B* and *C*).

Closed time frequency histograms were fitted best by multiple exponential components

Three exponential components were required to fit best each of the short and long closed time frequency histograms. For each distribution, the exponential components with the shortest to the longest time constants were designated components 1, 2 and 3, respectively. For each closed time analysis method, components 1 and 2 in the short closed time distributions (Table 3(A)) were similar at all concentrations (0·5, 1 and 2 μM). In the short closed time distribution of the main-conductance state, the two shortest components (1 and 2) overlapped at each concentration and had mean time constants of $0{\cdot}16 \pm 0{\cdot}01$ and $1{\cdot}22 \pm 0{\cdot}35$ ms, respectively. Similarly for the sub-conductance state, the two shortest components (1 and 2) of the short closed time distributions overlapped at each concentration and had mean time constants of $0{\cdot}17 \pm 0{\cdot}06$ and $1{\cdot}40 \pm 0{\cdot}20$ ms, respectively. As anticipated, the two shortest components in the short closed time distributions of all closings overlapped and were $0{\cdot}16 \pm 0{\cdot}03$ and $1{\cdot}15 \pm 0{\cdot}21$ ms, respectively. The time constant of the third component varied for the closings between main-conductance state and closings between sub-conductance state openings (Table 3(A)). However, the third component in the distribution of closings between both conductance states decreased with concentration (0·5–2 μM) from 30·3 to 13·6 ms. The relative proportion of the components showed no consistent trend.

Time constants found in the long closed time frequency distributions varied with method of analysis (Table 3(B)). In each method of closed time analysis, the first component time constants tended to decrease with increased glycine concentration. The first component was generally similar to the third component of the short closed time distribution at each concentration and method of analysis (compare τ_3 in Table 3(A) to τ_1 in Table 3(B)). The second component in the distribution of closures between main-conductance state openings decreased from 122 to 65 ms as glycine concentration was increased from 0·5 to 2 μM. The third component decreased from 717 to 557 ms. As glycine concentration was increased, the relative proportion of the first component decreased from 0·41 to 0·21, while the sum of the latter two components increased from 0·59 to 0·89. Similar to the main-conductance state, the second component in the distribution of closures between sub-conductance state openings decreased from 285 to 108 ms as glycine concentration was increased from 0·5 to 2 μM. The third component decreased from 819 to 488 ms. The relative proportion of the third component increased from 0·27 to 0·55 while the sum of the first two components decreased from 0·83 to 0·45. The ranges of component 3 of the main- and sub-conductance state long closed time constants were overlapping. However, the values for component 2 at each concentration were shorter for the main-conductance state compared to the sub-conductance state. The two longest time constants obtained for the closures between both main- and sub-conductance state openings

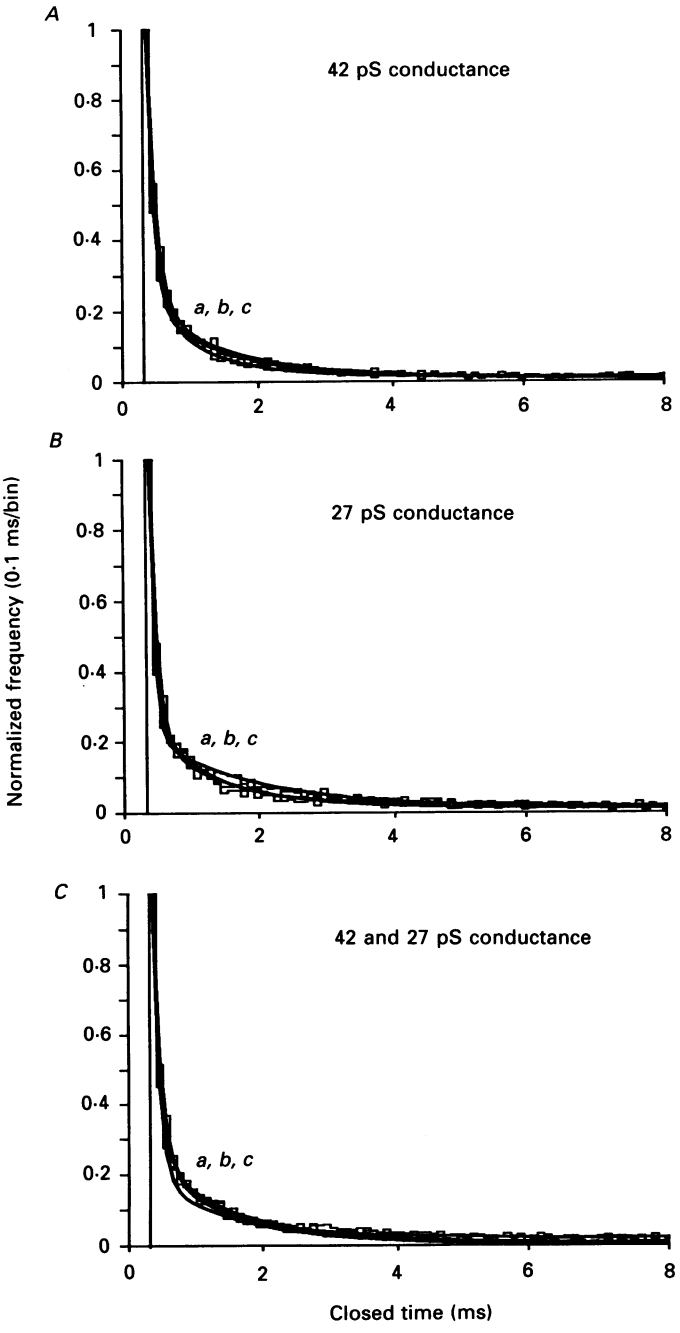

Fig. 6. Short closed times determined by three different methods (see text) were placed into frequency histograms and were fitted with three exponential components. In *A*, closed times were between main-conductance state openings and were assumed to be independent of sub-conductance state openings. In *B*, closed times were between sub-conductance state openings and were assumed to be independent of main-conductance

showed no consistent trend and ranged from 70 to 92 ms for component 2 and ranged from 312 to 522 ms for component 3 (Table 3(B)). The relative proportions of the components also showed no consistent trend.

It should be noted that validity of the longer time constants is questionable since channel activity in a patch could not be proven to be due to a single glycine receptor channel. Also, the effect of possible receptor desensitization cannot be assessed at the present time. It is difficult to interpret the relative contribution of the exponential components between short and long closed times since currently we are unable to analyse the presence of several exponential time constants in data ranging over several orders of magnitude. However, since the frequency of occurrence of multiple channel openings remained similar at each concentration, the observed increase in opening frequency with glycine concentration suggests that there was an overall increase in proportion of short duration closures and/or a decrease in dwell times in long duration closed states.

Burst properties

Bursts were defined as one or more openings separated by closings greater than t_c. At both conductance levels, a value for t_c was calculated for each closed time analysis method (see Methods). Since the two shortest time constants in the distributions of short closed times were concentration-invariant, a t_c was determined between the second and the third time constants in the closed time distributions for each concentration and for each closed time analysis method. Due to the invariance of the first two components, the calculated t_c varied little and a common t_c was selected for both main- and sub-conductance state openings. The solutions resulted in a mean t_c of 2·5 ms for both the main- and sub-conductance state openings.

As glycine concentration was increased, channel openings occurred more frequently in bursts (Figs 2, 3 and 4). As glycine concentration was increased (0·5–2 μM), the frequency of bursts of both conductance states increased from 2·8 to 5·7 bursts per second. The mean interburst closed times decreased from 357 to 175 ms. The frequency of bursts of the main-conductance state increased from 1·5 to 2·5 bursts per second, and the mean interburst closed time decreased from 667 to 400 ms (Table 4). Similarly for the sub-conductance state, the frequency of bursts increased from 1·3 to 3·2 bursts per second, and the mean interburst closed time decreased from 769 to 313 ms (Table 4).

Mean burst duration increased with glycine concentration (0·5–2 μM) from 6·4 to 13·9 ms for the main-conductance state and 2·7 to 5·6 ms for the sub-conductance state (Table 4). When corrected (see Table 4 legend), mean burst duration increased from 6·7 to 13·4 ms for the main-conductance state and from 3·6 to 7·8 ms for the sub-conductance state as glycine concentration was increased. Mean burst durations for each conductance state were stationary and varied little ($0·7 \pm 7·3$ %) when the data at each concentration were divided into twelve consecutive 5 s periods and analysed from the start of glycine application. For all bursts, the mean percentage of time

state openings. In *C*, closed times were between both main- and sub-conductance state openings. Short closed times for glycine at 0·5 (*a*), 1 (*b*) and 2 (*c*) μM were put into 0·1 ms bins and displayed for clarity over a range from 0·3 to 8 ms. Histograms were normalized and overlaid. Curves were drawn according to the fits (see text and Table 3).

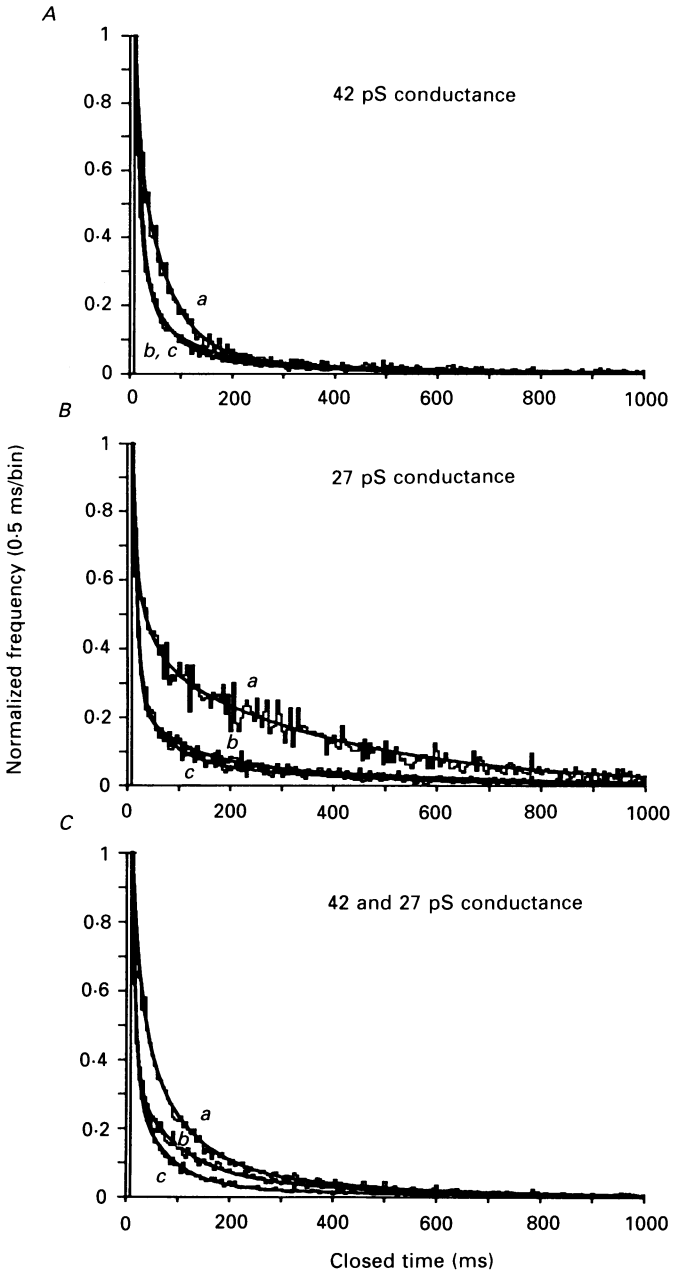

Fig. 7. Long closed times determined by three different methods (see text) were placed into frequency histograms and were fitted with three exponential components. In *A*, closed times were between main-conductance state openings and were assumed to be independent of sub-conductance state openings. In *B*, closed times were between sub-conductance state openings and were assumed to be independent of main-conductance state openings. In *C*, closed times were between both main- and sub-conductance state openings. Long closed times for 0·5 (*a*), 1 (*b*) and 2 (*c*) μM-glycine were put into 5 ms bins and displayed for clarity over a range from 15 to 1000 ms. Histograms were normalized and overlaid. Curves were drawn according to the fits (see text and Table 3).

TABLE 3. Glycine receptor main- and sub-conductance: short and long closed time constants and relative areas

(A) Short closed time constants and relative areas

[Glycine] (μM)	τ_1	τ_2	τ_3	a_1	a_2	a_3
			42 pS main-conductance state			
0·5	0·15 (0·10–0·23)	0·86 (0·34–2·10)	27·1 (17·8–44·3)	0·33 (0·17–0·49)	0·18 (n.d.–0·26)	0·49 (0·42–0·54)
1	0·15 (0·13–0·18)	1·24 (0·95–1·62)	16·1 (14·0–19·2)	0·41 (0·32–0·49)	0·29 (0·24–0·33)	0·31 (0·27–0·34)
2	0·17 (0·13–0·22)	1·55 (1·04–2·36)	23·2 (17·0–43·8)	0·37 (0·26–0·48)	0·31 (0·24–0·38)	0·32 (0·28–0·36)
			27 pS sub-conductance state			
0·5	0·16 (0·08–0·30)	1·20 (0·39–4·01)	27·5 (14·5–42·8)	0·34 (0·09–0·58)	0·25 (0·10–0·39)	0·41 (0·34–0·48)
1	0·23 (0·13–0·49)	1·40 (0·53–3·74)	12·9 (10·9–16·0)	0·29 (0·14–0·43)	0·24 (0·11–0·36)	0·48 (0·40–0·55)
2	0·12 (0·09–0·14)	1·61 (1·29–2·01)	15·0 (13·4–17·5)	0·34 (0·22–0·45)	0·36 (0·31–0·40)	0·31 (0·28–0·34)
			42 and 27 pS conductance states			
0·5	0·15 (0·12–0·19)	0·92 (0·48–1·76)	30·3 (20·1–47·8)	0·31 (0·20–0·41)	0·18 (0·12–0·23)	0·51 (0·42–0·62)
1	0·20 (0·16–0·28)	1·37 (0·85–2·20)	16·1 (7·97–46·8)	0·38 (0·29–0·49)	0·29 (0·22–0·37)	0·33 (n.d.–0·44)
2	0·20 (0·16–0·24)	1·31 (0·91–1·90)	13·6 (7·88–18·3)	0·39 (0·31–0·48)	0·29 (0·23–0·35)	0·32 (0·21–0·37)

(B) Long closed time constants and relative areas

[Glycine] (μM)	τ_1	τ_2	τ_3	a_1	a_2	a_3
			42 pS main-conductance state			
0·5	39·3 (28·6–55·9)	122·0 (79·1–187)	717 (565–1024)	0·41 (0·32–0·49)	0·34 (0·22–0·45)	0·25 (0·21–0·29)
1	10·5 (7·24–14·9)	94·3 (73·4–122)	700 (508–1973)	0·28 (0·23–0·33)	0·56 (0·47–0·65)	0·16 (0·13–0·20)
2	9·3 (5·35–15·1)	64·9 (47·6–91·1)	557 (492–637)	0·21 (0·15–0·26)	0·40 (0·31–0·49)	0·39 (0·34–0·44)
			27 pS sub-conductance state			
0·5	18·8 (n.d.–n.d.)	285 (240–330)	819 (n.d.–3754)	0·06 (0·05–0·12)	0·67 (0·50–0·80)	0·27 (n.d.–n.d.)
1	9·84 (6·25–15·1)	134 (96·4–184)	762 (611–1218)	0·23 (0·18–0·28)	0·47 (0·36–0·57)	0·31 (0·26–0·35)
2	8·31 (5·64–11·9)	108 (74·7–164)	488 (451–531)	0·18 (0·15–0·21)	0·27 (0·20–0·34)	0·55 (0·49–0·61)
			42 and 27 pS conductance states			
0·5	18·1 (12·2–27·2)	91·8 (78·8–108)	395 (368–425)	0·13 (0·10–0·16)	0·48 (0·43–0·54)	0·39 (0·34–0·44)
1	8·07 (5·94–10·8)	70·2 (57·8–86·5)	522 (467–585)	0·24 (0·21–0·28)	0·47 (0·41–0·53)	0·29 (0·25–0·32)
2	6·98 (5·46–8·80)	82·2 (71·2–95·6)	312 (295–328)	0·16 (0·14–0·18)	0·35 (0·32–0·39)	0·49 (0·45–0·53)

Time constants (τ_i) and relative areas (a_i) of exponential components fitted to short (A) and long (B) closed time frequency histograms (see Figs 6 and 7) for glycine (0·5, 1 and 2 μM). Closed times were determined by three different methods (see text for details). Components 1–3 corresponded to exponential components with the shortest to the longest time constants, respectively, in each histogram distribution. Ranges in parentheses represent likelihood intervals ($m = 2$). n.d. are ranges that could not be determined.

open within a burst changed little with concentration, varying from 95·4 to 96·4% for the main-conductance state and 92·3 to 94·8% for the sub-conductance state. Similarly, the mean intraburst closed time varied little with concentration and ranged from 0·52 to 0·57 ms for the main-conductance state and 0·62 to 0·69 ms for the sub-conductance state. Mean intraburst closed durations of each conductance

TABLE 4. Glycine receptor main- and sub-conductance states: burst properties

	Conductance					
	42 pS			27 pS		
Glycine concentration (μM)	0·5	1·0	2·0	0·5	1·0	2·0
Bursts frequency (s^{-1})	1·5	2·2	2·5	1·3	1·4	3·2
Mean interburst closed time (ms)	667	455	400	769	714	313
Mean burst duration (ms)	6·4	11·0	13·9	2·7	4·5	5·6
Corrected mean burst duration (ms)	6·7	10·8	13·4	3·6	4·5	7·8
Percentage of time open (%)	96·4	95·6	95·4	94·8	92·4	92·3
Mean intraburst closed time (ms)	0·53	0·57	0·52	0·62	0·66	0·69
Mean number of openings/burst	1·43	1·84	1·95	1·22	1·51	1·63
Number of bursts	6884	8010	7537	6200	5086	9375

Burst frequency, mean interburst closed time, mean burst duration, percentage of time open within a burst and number of bursts were derived from detected 42 pS main-conductance and 27 pS sub-conductance state bursts and openings and closings within bursts (see Methods). Bursts were separated by closures greater than 2·5 ms. Percentage open within a burst was calculated by taking the percentage of the total open time in a burst divided by the total time in a burst (total open time plus total intraburst closed time). Corrected mean burst duration was calculated by taking the sum of the relative area of each exponential component in the burst duration histogram multiplied by the time constant of the component (corrected mean burst duration $= a_1\tau_1 + a_2\tau_2 + a_3\tau_3$).

state were stationary and varied little ($2{\cdot}2 \pm 1{\cdot}9\%$) when the data at each concentration were divided into twelve consecutive 5 s epoches and analysed from the start of glycine application. The probability for each conductance state to burst with more than one opening in succession increased with concentration. The mean number of openings per burst increased from 1·43 to 1·95 for bursts of the main-conductance state and from 1·22 to 1·63 for bursts of the sub-conductance state. Thus at each concentration, bursts of main-conductance state openings were more likely to be evoked, and the bursts contained a greater mean number of openings.

Burst duration frequency histograms were fitted best by multiple exponential components

As with open and closed duration histograms, burst duration frequency histograms were obtained by pooling burst durations from several patches at each concentration. For each conductance state, burst durations were binned with a bin width of 0·5 ms and a range of 0·5–150 ms. At each conductance level, there was a shift in the burst duration distribution to longer durations as glycine concentration increased, consistent with an increase in the relative frequency of occurrence of longer bursts (Fig. 8). At each concentration, bursts of main-conductance state openings (Fig. 8*A*) were generally longer than bursts of sub-conductance state openings (Fig. 8*B*).

To determine the basis for the increased relative frequency of occurrence of longer bursts with increasing concentration of glycine, burst duration frequency histograms were fitted with multiple exponential components. For the main-conductance state, burst duration frequency histograms at all three glycine concentration were fitted

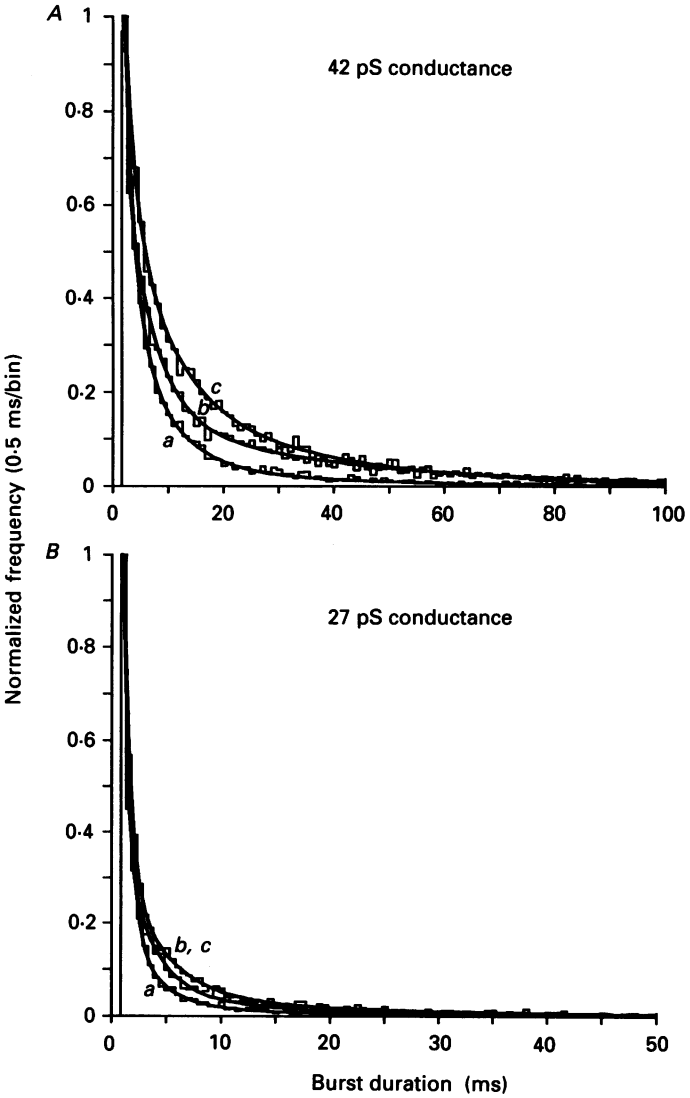

Fig. 8. Burst duration frequency histograms of the main-conductance (*A*) and sub-conductance (*B*) state were fitted with multiple exponential components. Burst durations evoked by 0·5 (*a*), 1 (*b*) and 2 (*c*) μM-glycine were put into 0·5 ms bins and displayed for clarity over a range of 1–100 ms or 1–50 ms. Distributions were normalized and overlaid. Curves were drawn according to the fits (see text and Table 5). The numbers of bursts in the histograms at each concentration are the same as those provided in Table 4.

best with four exponential components. Components 1–4 represented exponential components with the shortest to the longest time constants. The time constants of the four components varied little with glycine concentration (Table 5(A)). Components 1–4 averaged $0{\cdot}78 \pm 0{\cdot}11$, $2{\cdot}50 \pm 0{\cdot}27$, $9{\cdot}14 \pm 1{\cdot}17$ and $28{\cdot}2 \pm 5{\cdot}5$ ms, respectively. As glycine concentration increased, the relative area of component 1

TABLE 5. Glycine receptor main- and sub-conductance states: burst duration time constants and relative areas

(A) Time constants

[Glycine] (μM)	τ_1	τ_2	τ_3	τ_4
		42 pS main-conductance state		
0·5	0·71 (0·49–1·01)	2·49 (2·08–3·03)	8·99 (6·62–11·2)	33·6 (23·4–166)
1	0·90 (0·43–1·65)	2·77 (2·09–3·77)	8·05 (6·91–9·47)	22·5 (20·6–24·4)
2	0·72 (n.d.–n.d.)	2·23 (1·58–3·10)	10·4 (7·41–14·1)	28·5 (25·1–28·5)
		27 pS sub-conductance state		
0·5	0·67 (0·62–0·77)	4·27 (3·48–5·21)	25·6 (16·2–93·0)	—
1	0·42 (0·36–0·50)	3·75 (3·23–4·37)	18·5 (15·1–22·6)	—
2	0·63 (0·50–0·79)	4·30 (3·57–5·22)	24·6 (21·5–27·9)	—

(B) Relative areas

[Glycine] (μM)	a_1	a_2	a_3	a_4
		42 pS main-conductance state		
0·5	0·21 (0·17–0·25)	0·42 (0·37–0·46)	0·28 (0·21–0·34)	0·09 (0·06–0·12)
1	0·09 (0·06–n.d.)	0·19 (0·15–0·19)	0·43 (0·37–0·47)	0·30 (0·26–0·34)
2	0·02 (n.d.–n.d.)	0·32 (0·25–0·37)	0·34 (0·26–0·42)	0·32 (0·25–0·38)
		27 pS sub-conductance state		
0·5	0·61 (0·57–0·64)	0·33 (0·28–0·37)	0·07 (0·05–0·09)	—
1	0·39 (0·35–0·42)	0·47 (0·43–0·52)	0·14 (0·11–0·17)	—
2	0·33 (0·29–0·37)	0·43 (0·37–0·48)	0·24 (0·19–0·29)	—

Time constants (τ_i) and relative areas (a_i) of exponential components fitted to burst duration frequency histograms (see Fig. 8) for the 42 pS main-conductance and 27 pS sub-conductance states evoked by glycine (0·5, 1 and 2 μM). For the 42 pS main-conductance state, components 1–4 corresponded to the exponential components with the shortest to the longest time constants, respectively. For the 27 pS sub-conductance state, components 1–3 corresponded to the exponential components with the shortest to the longest time constants, respectively. Ranges in parentheses represent likelihood intervals ($m = 2$).

was reduced from 0·21 to 0·02, and the relative areas of components 2, 3 and 4 were increased from 0·79 to 0·98 (Table 5(B)).

For the sub-conductance state, the burst duration frequency histograms for all three glycine concentrations were fitted best with three exponential components. Components 1–3 represented exponential components with the shortest to the longest time constants (Table 5). The time constant of the three components varied little with glycine concentration. Components 1–3 averaged $0{\cdot}58 \pm 0{\cdot}14$, $4{\cdot}11 \pm 0{\cdot}31$ and $22{\cdot}9 \pm 3{\cdot}9$ ms, respectively (Table 5(A)). As glycine concentration increased, the relative area of component 1 decreased from 0·61 to 0·33, while the relative area of

components 2 and 3 increased from 0·39 to 0·67 (Table 5(B)). Thus, increasing glycine concentration resulted in a shift in the burst duration frequency histogram to longer durations by reducing the relative proportion of shorter bursts and by increasing the relative proportion of longer bursts.

DISCUSSION

Conductance

At −75 mV in symmetrical chloride solutions, two predominant current amplitudes were evoked by glycine with average conductances of about 42 and 27 pS. The dominant or main-conductance level was 42 pS. The chord conductances of the main- and sub-conductance states were the same when evoked by glycine concentrations from 0·5 to 2 μM. Thus, the increased current produced by increased glycine concentration was due to an increase in the frequency of channel opening, a change in the relative occurrence of the main- and sub-conductance state and/or a change in the gating properties of the channel.

The conductances measured for mouse spinal cord neurones in culture were similar to those reported for glycine-gated single channels from other mammalian neurones (Sakmann *et al.* 1983; Hamill *et al.* 1983; Bormann *et al.* 1987; Smith *et al.* 1989). The greater frequency of occurrence observed for the 42 pS state was also similar, but this difference has been disputed (Smith *et al.* 1989). It has been suggested that since glycine and GABA activated channel openings to conductances that form a geometric progression, a receptor composed of a cluster of coupled, identical ion-conducting pores was an unlikely explanation of multiple conductance states (Smith *et al.* 1989). Studies of hybrid *Torpedo* and bovine nACh receptor subunits and cloned subunits of the bovine brain $GABA_A$ receptor have shown that subunit composition might determine the predominant conductance state attained when the receptor is activated (Sakmann, Methfessel, Mishina, Takahashi, Takai, Kurasaki, Fukuda & Numa, 1985; Mishina, Takai, Imoto, Noda, Takahashi, Numa, Methfessel & Sakmann, 1986; Moss, Smart, Porter, Nayeem, Devine, Stephenson, Macdonald & Barnard, 1990). Nicotinic ACh receptors composed of $\alpha_2\beta\delta\epsilon$ subunits have been reported to have a larger conductance and shorter mean channel open time than nACh receptors composed of $\alpha_2\beta\gamma\delta$ subunits (Mishina *et al.* 1986). $GABA_A$ receptors composed of $\alpha_1\beta_1$ subunits have a smaller conductance and have a shorter mean channel open time than the native receptor which might be composed of α, β and γ subunits (Prichett, Sontheimer, Shivers, Ymer, Kettenmann, Schofield & Seeburg, 1989; Moss *et al.* 1990). Since the glycine receptor channel might be formed by a pentamer of at least two different subunits of unknown stoichiometry (Langosch *et al.* 1988; Schmieden *et al.* 1989), it is possible that the different conductance states evoked by glycine might represent different combinations of isoforms or physical configurations of the glycine receptor subunits.

Transitions from the 42 pS main-conductance state to the 27 pS sub-conductance state and from the 27 pS sub-conductance state to the 42 pS main-conductance state without an observed closing were observed. Transitions from the sub-conductance to the main-conductance state occurred approximately eight times more frequently than transition from the main-conductance state to the sub-conductance state. Over

the glycine concentration range (0·5–2 μM), observed transitions from the main-conductance to the sub-conductance state averaged about 30 times more frequent than expected for independent channels while observed transitions from the sub-conductance to the main-conductance state averaged about 230 times more frequent than expected. Although different and independent 42 and 27 pS channels may have been present, these results suggest that at least some of the observed 42 and 27 pS openings were from a single receptor channel. These fast transition conductance changes may have been a result of conformational changes or molecular substitution in a single receptor/channel or, less likely, spontaneous re-configuration or re-assembly of the receptor subunits. Occasionally, prolonged periods of channel activity contained only one conductance state. It might be possible that during these periods, a single channel may stably transform from one conductance state to another as a result of re-configuration or re-assembly of the receptor subunits. Conductance state transitions also might be explained by the possibility that multiple channels representing different conductance states can couple to each other, and thus possibly regulate gating. For example, receptor coupling via disulphide bonds has been speculated as a means for nACh receptor desensitization (Tolliver & Pellmar, 1988). Further study, perhaps with cloned receptor subunits, is required to draw conclusions about glycine receptor subunit composition and channel kinetics.

Open properties

When patches were exposed to glycine at low concentrations (0·5–2 μM), opening frequency and mean open time for both conductance states increased as glycine concentration increased. Since the three exponential component open time constants found in the frequency distribution of main- and sub-conductance state open durations did not change with glycine concentration, each conductance state might be gated open to at least three open states of different mean durations. The open states of each conductance state differed, however, in that the larger conductance state adopted a more stable, generally longer duration open conformation and was gated open more frequently. The differences in permeabilities and open durations of the two conductance states suggest that perhaps the subunit configuration or the protein conformation giving rise to the main-conductance state is different from that of the sub-conductance state.

Evidence to date suggests that at least two and most likely three glycine molecules must be bound for complete activation of the mammalian glycine receptor (Young & Snyder, 1974*b*; Sakmann *et al.* 1983; Langosch *et al.* 1988; Smith *et al.* 1989; Schmieden *et al.* 1989). Whether or not a single bound state can produce channel opening remains unclear (Cull-Candy *et al.* 1981; Sine & Steinbach, 1984, 1986; Colquhoun & Sakmann, 1985), but evidence from studies of nACh and $GABA_A$ receptor channels activated by low concentrations of agonist indicate that a singly liganded receptor might open briefly (Dionne, Steinbach & Stevens, 1978; Colquhoun & Sakmann, 1985; Jackson, 1988; Macdonald *et al.* 1989; Twyman *et al.* 1990). At the lowest concentration (0·5 μM), glycine evoked openings that were predominantly to the short-lived open state for both conductance states. With increased glycine concentration, the frequency of brief open state openings decreased compared to the frequency of longer openings. This suggests that a portion of openings due to the brief open states might represent openings of a singly liganded glycine receptor.

As glycine concentration was increased, openings from the two longer open states increased in frequency and in relative proportion compared to the briefest open state, suggesting that these states occurred after glycine binding. Openings to the longer states, therefore, probably occurred primarily when the glycine receptor was fully (doubly or perhaps triply) liganded. The invariance of the open time constants with concentration suggests that the longer open states were not directly connected or that the rates between them were very low. Thus, the observed increased current with glycine concentration was due to an increased probability of opening of both conductance states and opening of both conductance states to more stable, long duration open states. The majority of current evoked, however, was through the main-conductance state.

Notably, the main- and sub-conductance states differed for the behaviour of component 2 relative to component 3. For the main-conductance state, the relative proportion due to component 2 decreased compared to the proportion due to component 3 at the highest glycine concentration (2 μM). For the sub-conductance state, the proportions due to component 2 and 3 both increased by approximately the same amount (Table 2). This disparity suggests there might be a difference in the sequential binding of glycine to activate each conductance state.

The kinetic properties of the glycine receptor channel were similar to those found for the $GABA_A$ and nACh receptor channels. The nACh and $GABA_A$ receptors both appear to require binding of at least two agonist molecules for complete activation. Both receptor types demonstrate an increase in opening frequency and open duration when activated by low concentrations of agonist (Dionne *et al.* 1978; Takeda & Trautmann, 1984; Labarca, Montal, Lindstrom & Montal, 1985; Mathers, 1985; Colquhoun & Sakmann, 1985; Hestrin, Korenbrot & Maricq, 1987; Jackson, 1988; Macdonald *et al.* 1989; Twyman *et al.* 1990). Since the α-subunit of the nACh receptor, the α- and β-subunits of the $GABA_A$ receptor and the α-subunit of the glycine receptor have shown significant sequence similarity (Schofield *et al.* 1987), it can be speculated that some of the similar amino acid domains of this receptor superfamily confer these general gating characteristics of ligand-gating receptor channels.

Closed properties

Glycine receptor channel closed properties also varied with concentration and with method of analysis. The time constants of the two shortest components were not significantly different whether the closures between openings were assumed to be dependent or independent of open conductance. Three longer closed dwell times were apparent suggesting that at least five closed time constants exist. It is difficult to assign the longer closed component time constants to specific closed states since it was not possible to record from patches which definitely contained a single glycine receptor channel and the effects of desensitization on long extraburst closed durations could not be controlled. Since opening frequency decreased over time, the longest component indeed might be an additional time constant due to the presence of desensitization or it may be due to the presence of one or more channels in the patch. However, since care was taken to include only recordings from patches which had minimal (less than 1–3%) occurrence of multiple openings, it is likely that multiple long closed states exist.

The concentration invariance of the two shortest time constants suggests the presence of at least two brief closed states which probably occurred after glycine binding. The longer time constants varied with concentration, suggesting that the closed states that gave rise to these closed time constants occurred prior to the receptor becoming fully liganded. Concentration-invariant short closed time constants have also been observed in nACh receptors from clonal BC3H-1 cells (Sine & Steinbach, 1986) and $GABA_A$ receptors from mouse spinal cord neurones in culture (Macdonald *et al.* 1989). For the $GABA_A$ receptor, analysis of intraburst kinetics revealed that two concentration-invariant closed time constants represented closed states located distal to open states (Twyman *et al.* 1990). Entry into these closed states occurred after binding of agonist and gating to an open state. Given the similarity of these ligand-gated receptors, the kinetic gating scheme for the brief closed states for glycine might be similar to the scheme for the $GABA_A$ receptor. The physical origin of these brief closed states is uncertain, but the closures might represent anions plugging the pore causing channel block or intrinsic relaxations of the channel protein causing brief interruptions of current flow (Sine & Steinbach, 1986; Lauger, 1988; Twyman *et al.* 1990). To further speculate on the location of glycine binding relative to closed states, more extensive analysis of intraburst kinetics is required and is beyond the scope of the present paper.

Burst properties

Similar to the nACh and $GABA_A$ receptors, low concentrations of glycine (0·5–2 μM) evoked openings to each conductance state that were grouped into bursts (Sakmann *et al.* 1983; Hamill *et al.* 1983; Colquhoun & Sakmann, 1985; Hestrin *et al.* 1987; Jaramillo & Schuetze, 1988; Macdonald *et al.* 1989). Both burst frequency and mean burst duration of both conductance states increased with glycine concentration, but the percentage open within a burst and the mean intraburst closed time did not vary with concentration. These burst properties were similar to those of the $GABA_A$ receptor channel and suggest that they were produced by fully bound glycine receptor channels and the open and closed states that produced bursts were distal to glycine-binding steps in a microscopic reaction scheme (Macdonald *et al.* 1989; Twyman *et al.* 1990).

The presence of at least three open and two intraburst closed states indicated that frequency distributions of burst durations might contain a maximum of five exponential components for each conductance (Colquhoun & Hawkes, 1982). However, only four predominant components for the main-conductance state and three components for the sub-conductance state were resolved. For both conductance states, an increase in mean burst duration with increased glycine concentration was achieved by a decrease in the relative proportion of bursts with short durations and an increase in the relative proportion of bursts with longer durations. For the main-conductance state, the briefest open component and the shortest burst duration component had similar time constants, and as glycine concentration increased, the relative frequency of the brief open component and short bursts decreased. Similar results were found for the sub-conductance state. Thus, it was likely that the short bursts were produced primarily by single openings of the brief open component. The longer time constants found in the burst duration histograms were greater than the

time constants found in the open time histograms. In addition, the relative proportion due to the two longest components in the burst duration histograms increased with increased glycine concentration similar to the two longest components of the open time histograms. Thus, the longer components in the burst duration histograms were produced primarily by groups of two or more openings to more stable, longer duration open components. Bursts of these openings occurred with greater frequency and higher probability relative to shorter duration bursts when the receptor was fully liganded. Further conclusions concerning burst properties would require a more detailed analysis of intraburst kinetics. However, the similarity in burst properties for both the main- and sub-conductance stages suggests that the mechanism for activation of bursts for both of these conductance states was similar. These changes in burst duration components with low concentrations of glycine are similar to those found for the $GABA_A$ receptor activated by low concentration of GABA (Macdonald *et al.* 1989), and are consistent with a similar mechanism for gating of glycine and $GABA_A$ receptors.

Due to limited frequency response, the reported mean channel durations measured by fluctuation noise analysis of receptor currents probably represented bursts of openings. Using ionophoretically applied glycine on mouse spinal cord or sensory neurones, estimated channel durations ranged from 5 to 13 ms (Nicholl, Padjen & Barker, 1976; Barker, McBurney & MacDonald, 1982). Although the variability in channel durations may be due to the unknown concentrations of glycine applied by ionophoresis, the reported results compare well to the mean burst durations evoked by low concentrations of glycine in the present study (Table 4). As demonstrated by the present study, mean burst durations were dependent on glycine concentration, but the exponential time constants of burst durations did not change with concentration. The observed increase in mean burst durations was due to increases in relative proportions of exponential components with longer time constants.

Initial kinetic model

The durations of the observed channel open and closed times might be interpreted as sojourns in various states of a kinetic model represented by an unbound receptor, liganded receptor without channel opening and liganded receptor with channel opening (Colquhoun & Hawkes, 1982). Since the open, closed and burst properties of the 42 pS main-conductance state were similar to those found for the nACh and $GABA_A$ receptor channels, the following preliminary scheme for the glycine receptor

$$\begin{array}{lcccl} 3A+R & \underset{k_{-a1}}{\overset{k_{+a1}}{\rightleftharpoons}} & 2A+AR & \underset{k_{-a2}}{\overset{k_{+a2}}{\rightleftharpoons}} & A+A_2R \quad \underset{k_{-a3}}{\overset{k_{+a3}}{\rightleftharpoons}} \quad A_3R \qquad \text{Closed states} \\ \beta_1 \downarrow \uparrow \alpha_1 & & \beta_2 \downarrow \uparrow \alpha_2 & & \beta_3 \downarrow \uparrow \alpha_3 \\ 2A+AR^* & \underset{k_{-1}}{\overset{k_{+1}}{\rightleftharpoons}} & A+A_2R^* & \underset{k_{-2}}{\overset{k_{+2}}{\rightleftharpoons}} & A_3R^* \qquad \text{Open states} \end{array}$$

Scheme 1

main-conductance state is proposed. The kinetic scheme is composed of three open states, four closed states and three agonist binding sites, where A represents an agonist molecule, R a receptor and * an open state.

The open states corresponding to components 1, 2 and 3 are represented by the bound open conformations AR*, A_2R^* and A_3R^*, respectively. The microscopic transition rate constants between the states are designated α_i, β_i and k_i. Due to the concentration invariance of the open time constants, the transition rates between the open states will be considered to be small but are presented for completeness. In this model, a singly liganded receptor might open to the brief open state (AR*). The above scheme is consistent with the observation that as glycine concentration increased, the proportion of state AR* decreased relative to states A_2R^* and A_3R^*. Also, the proportion of component 2 decreased relative to the proportion of component 3 as concentration was increased. This is consistent with the reaction scheme being driven further right to A_3R^* openings as glycine concentration was increased. A burst might occur between an open state and its associated closed state. However, bursts of openings involving the doubly or triply liganded states A_2R^* and A_3R^* would contribute the majority of current. This was suggested by the increase in relative proportion of long duration openings and bursts as concentration was increased. The kinetic scheme must be considered an initial working model which is likely to be incomplete. The model is testable however, and the similarities to the $GABA_A$ receptor noted above suggest that the gating scheme might be more complex (Macdonald *et al.* 1989; Twyman *et al.* 1990). Indeed, as has been found for the nACh and GABA receptors, the concentration invariance of brief closed time constants suggests the presence of closed states located distal to channel opening (Sine & Steinbach, 1986; Twyman *et al.* 1990). Currently, a distal closed state has not been firmly established, and therefore it was not incorporated into the above scheme.

Since activation properties of the 27 pS sub-conductance state are similar, the above scheme might be proposed also as a preliminary gating scheme for the glycine sub-conductance state. However, since there are suggestions that for the $GABA_A$ receptor different subunit compositions might open to similar but different predominant conductance states (Moss *et al.* 1990), an independent gating scheme for the glycine sub-conductance would not be unreasonable. Closing energies for GABA and glycine channels have been shown to be similar (Mathers & Barker, 1981) and the closing kinetics of the glycine 27 pS conductance state appear to be similar to the

$$2A + R \underset{k_{-a1}}{\overset{k_{+a1}}{\rightleftharpoons}} A + AR \underset{k_{-a2}}{\overset{k_{+a2}}{\rightleftharpoons}} A_2R \underset{k_{-a3}}{\overset{k_{+a3}}{\rightleftharpoons}} A_2R' \qquad \text{Closed states}$$

$$\beta_1 \downarrow \alpha_1 \qquad \beta_2 \downarrow \alpha_2 \qquad \beta_3 \downarrow \alpha_3$$

$$A + AR^* \underset{k_{-1}}{\overset{k_{+1}}{\rightleftharpoons}} A_2R^* \underset{k_{-2}}{\overset{k_{+2}}{\rightleftharpoons}} A_2R'^* \qquad \text{Open states}$$

Scheme 2

closing kinetics of the $GABA_A$ 27 pS main-conductance state (R. E. Twyman, C. J. Rogers, N. Porter & R. L. Macdonald, unpublished). Since full activation of the GABA receptor main state requires binding of two agonist molecules, a similarity in the gating of the 27 pS conductance states would suggest the binding of only two glycine molecules to evoke the 27 pS glycine sub-conductance state. A possible model for this conductance state incorporating three open states, four closed states and two agonist-binding sites is shown in scheme 2.

Again, the open states corresponding to components 1, 2 and 3 are represented by the bound open conformations AR*, A_2R^* and $A_2R'^*$, respectively. The transition rate constants between the states are designated α_i, β_i and k_i. Similar to scheme 1, the singly liganded receptor might open to AR* and the proportion of state AR* decreases with increased concentration of glycine. In contrast to the main-conductance state in scheme 1, the proportion of state A_2R^* does not decrease relative to state $A_2R'^*$ as glycine concentration is increased.

Cross-linking of affinity-purified glycine receptor preparations and studies of a homo-oligomer assembly of the α-subunit of the rat spinal cord glycine receptor indicate that perhaps the glycine receptor has a stoichiometry of $\alpha_3\beta_2$ and requires binding to all three α-subunits for full activation of the receptor (Langosch *et al.* 1988; Schmieden *et al.* 1989). It is speculated that a different stoichiometry, perhaps $\alpha_2\beta_2$ or $\alpha_2\beta_3$, or isoforms of the subunits, might predominantly produce the 27 pS sub-conductance state and might require only two glycine molecules for complete activation. The kinetic interrelationship of the multiple conductance states evoked by glycine is unclear and remains to be resolved.

The authors wish to thank Mrs Nancy Ciliax for technical assistance in the preparation and maintenance of cell cultures and Dr Carl Rogers for the computer system hardware set-up.

REFERENCES

AKAIKE, N. & KANEDA, M. (1989). Glycine-gated chloride current in acutely isolated rat hippocampal neurons. *Journal of Neurophysiology* **6**, 1400–1409.

APRISON, M. H. & WERMAN, R. (1965). The distribution of glycine in cat spinal cord and roots. *Life Sciences* **4**, 2075–2083.

BARKER, J. L. & MCBURNEY, R. M. (1979). GABA and glycine might share the same conductance channel on cultured mammalian neurones. *Nature* **277**, 234–236.

BARKER, J. L., MCBURNEY, R. M. & MACDONALD, J. F. (1982). Fluctuation analysis of neutral amino acid responses in cultured mouse spinal neurones. *Journal of Physiology* **322**, 365–387.

BARKER, J. L. & RANSOM, B. R. (1978). Amino acid pharmacology of mammalian central neurones grown in tissue culture. *Journal of Physiology* **280**, 331–354.

BECKER, C. M., HERMANS-BORGMEYER, I., SCHMITT, B. & BETZ, H. (1986). The glycine receptor deficiency of the mutant mouse spastic: evidence for normal glycine receptor structure and function. *Journal of Neuroscience* **6**, 1358–1364.

BETZ, H. & BECKER, C. M. (1988). The mammalian glycine receptor: biology and structure of a neuronal chloride channel protein. *Neurochemistry International* **13**, 137–146.

BLATZ, A. L. & MAGLEBY, K. L. (1986). Correcting single channel data for missed events. *Biophysical Journal* **49**, 967–980.

BORMANN, J., HAMILL, O. P. & SAKMANN, B. (1987). Mechanism of anion permeation through channels gated by glycine and γ-aminobutyric acid in mouse cultured spinal neurones. *Journal of Physiology* **385**, 243–286.

COLQUHOUN, D. & HAWKES, A. G. (1982). On the stochastic properties of bursts of single ion

channel openings and clusters of bursts. *Philosophical Transactions of the Royal Society* **B 300**, 1–59.

COLQUHOUN, D. & SAKMANN, B. (1985). Fast events in single-channel currents activated by acetylcholine and its analogues at the frog muscle end-plate. *Journal of Physiology* **369**, 501–557.

COLQUHOUN, D. & SIGWORTH, F. J. (1983). Fitting and statistical analysis of single-channel records. In *Single-Channel Recordings*, ed. SAKMANN, B. & NEHER, E., pp. 191–263. Plenum Press, New York.

CULL-CANDY, S. G., MILEDI, R. & PARKER, I. (1981). Single glutamate-activated channels recorded from locust muscle fibres with perfused patch electrodes. *Journal of Physiology* **321**, 195–210.

CURTIS, D. R., HOSLI, L. & JOHNSTON, G. A. R. (1968). A pharmacological study of the depression of spinal neurones by glycine and related amino acids. *Experimental Brain Research* **6**, 1–18.

CURTIS, D. R., HOSLI, L., JOHNSTON, G. A. R. & JOHNSTON, L. H. (1968). The hyperpolarization of spinal motoneurones by glycine and related amino acids. *Experimental Brain Research* **5**, 235–258.

DIONNE, V. E. & LIEBOWITZ, M. D. (1982). Acetylcholine receptor kinetics: a description from single-channel currents at snake neuromuscular junctions. *Biophysical Journal* **39**, 253–261.

DIONNE, V. E., STEINBACH, J. J. & STEVENS, C. F. (1978). An analysis of the dose–response relationship at voltage-clamped frog neuromuscular junctions. *Journal of Physiology* **281**, 421–444.

GOLD, M. R. & MARTIN, A. R. (1983). Analysis of glycine-activated inhibitory post-synaptic channels in brain-stem neurones of the lamprey. *Journal of Physiology* **342**, 99–117.

GRENNINGLOH, G., RIENITZ, A., SCHMITT, B., METHFESSEL, C., ZENSEN, M., BEREUTHER, K., GUNDELFINGER, E. D. & BETZ, H. (1987). The strychnine-binding subunit of the glycine receptor shows homology with nicotinic receptors. *Nature* **328**, 215–220.

HAMILL, O. P., BORMANN, J. & SAKMANN, B. (1983). Activation of multiple-conductance state chloride channels in spinal neurones by glycine and GABA. *Nature* **305**, 805–808.

HAMILL, O. P., MARTY, A., NEHER, E., SAKMANN, B. & SIGWORTH, F. J. (1981). Improved patch-clamp techniques for high-resolution current recording from cells and cell-free membrane patches. *Pflügers Archiv* **391**, 85–100.

HESTRIN, S., KORENBROT, J. L. & MARICQ, A. V. (1987). Kinetics of activation of acetylcholine receptors in a mouse muscle cell line under a range of acetylcholine concentrations. *Biophysical Journal* **51**, 449–455.

JACKSON, M. B. (1988). Dependence of acetylcholine receptor channel kinetics on agonist concentration in cultured mouse muscle fibres. *Journal of Physiology* **387**, 555–583.

JARAMILLO, F. & SCHUETZE, S. M. (1988). Kinetic differences between embryonic- and adult-type acetylcholine receptors in rat myotubes. *Journal of Physiology* **398**, 267–296.

LABARCA, P., MONTAL, M. S., LINDSTROM, J. & MONTAL, M. (1985). The occurrence of long openings in the purified cholinergic channel increases with acetylcholine concentration. *Journal of Neuroscience* **5**, 3409–3413.

LANGOSCH, D., LEO, T. & BETZ, H. (1988). Conserved quaternary structure of ligand-gated ion channels: the postsynaptic glycine receptor is a pentamer. *Proceedings of the National Academy of Sciences of the USA* **85**, 7394–7398.

LAUGER, P. (1988). Internal motions in proteins and gating kinetics of ionic channels. *Biophysical Journal* **47**, 469–478.

MACDONALD, R. L., ROGERS, C. J. & TWYMAN, R. E. (1989). Kinetic properties of the $GABA_A$ receptor main-conductance state of mouse spinal cord neurones in culture. *Journal of Physiology* **410**, 479–499.

MCMANUS, O. B., BLATZ, A. L. & MAGLEBY, K. L. (1987). Sampling, log binning, fitting, and plotting durations of open and shut intervals from single channels and the effects of noise. *Pflügers Archiv* **410**, 530–553.

MATHERS, D. A. (1985). Spontaneous and GABA-induced single channel currents in cultured murine spinal cord neurons. *Canadian Journal of Physiology and Pharmacology* **63**, 1228–1233.

MATHERS, D. A. & BARKER, J. L. (1981). GABA- and glycine-induced Cl^- channels in cultured mouse spinal neurons require the same energy to close. *Brain Research* **224**, 441–445.

MISHINA, M., TAKAI, T., IMOTO, K., NODA, M., TAKAHASHI, T., NUMA, S., METHFESSEL, C. & SAKMANN, B. (1986). Molecular distinction between fetal and adult forms of muscle acetylcholine receptor. *Nature* **321**, 406–411.

MOSS, S., SMART, T., PORTER, N., NAYEEM, N., DEVINE, J., STEPHENSON, F. A., MACDONALD, R. L. & BARNARD, E. A. (1990). Cloned GABA receptors are maintained in a stable cell line: allosteric and channel properties. *European Journal of Pharmacology* **189**, 77–88.

NICOLL, R. A., PADJEN, A. & BARKER, J. L. (1976). Analysis of amino acid responses on frog motoneurones. *Neuropharmacology* **15**, 45–53.

NOWAK, L. M., YOUNG, A. B. & MACDONALD, R. L. (1982). GABA and bicuculline actions on mouse spinal cord and cortical neurons in cell culture. *Brain Research* **224**, 155–164.

PFEIFFER, F., GRAHAM, D. & BETZ, H. (1982). Purification by affinity chromatography of the glycine receptor from rat spinal cord. *Journal of Biological Chemistry* **257**, 9389–9393.

PRICHETT, D. B., SONTHEIMER, H., SHIVERS, B. D., YMER, S., KETTENMANN, H., SCHOFIELD, P. R. & SEEBURG, P. H. (1989). Importance of a novel $GABA_A$ receptor subunit for benzodiazepine pharmacology. *Nature* **338**, 582–584.

SAKMANN, B., HAMILL, O. P. & BORMANN, J. (1983). Patch-clamp measurements of elementary chloride currents activated by the putative inhibitory transmitters GABA and glycine in mammalian spinal neurons. *Journal of Neural Transmission Supplementum* **18**, 83–95.

SAKMANN, B., METHFESSEL, C., MISHINA, M., TAKAHASHI, T., TAKAI, T., KURNASAKI, M., FUKUDA, K. & NUMA, S. (1985). Role of acetylcholine subunits in gating of the channel. *Nature* **318**, 538–543.

SCHMIEDEN, V., GRENNINGLOH, G., SCHOFIELD, P. R. & BETZ, H. (1989). Functional expression in Xenopus oocytes of the strychnine binding 48 kd subunit of the glycine receptor. *European Membrane Biology Organization Journal* **8**, 695–700.

SCHOFIELD, P. R., DARLISON, M. G., FUJITA, N., BURT, D. R., STEPHENSON, F. A., RODRIGUEZ, H., RHEE, L. M., RAMACHANDRAN, J., REALE, V., GLENCORSE, T. A., SEEBURG, P. A. & BARNARD, E. A. (1987). Sequence and functional expression of the $GABA_A$ receptor shows a ligand-gated receptor super-family. *Nature* **328**, 221–227.

SINE, S. M. & STEINBACH, J. H. (1984). Activation of a nicotinic acetylcholine receptor. *Biophysical Journal* **45**, 175–185.

SINE, S. M. & STEINBACH, J. H. (1986). Activation of acetylcholine receptors on clonal mammalian BC3H-1 cells by low concentrations of agonist. *Journal of Physiology* **373**, 129–162.

SMITH, S. M., ZOREC, R. & MCBURNEY, R. N. (1989). Conductance states activated by glycine and GABA in rat cultured spinal neurons. *Journal of Membrane Biology* **108**, 45–52.

TAKEDA, N. & TRAUTMANN, A. (1984). A patch-clamp study of the partial actions of tubocurarine on rat myotubes. *Journal of Physiology* **349**, 353–374.

TOLLIVER, J. M. & PELLMAR, T. C. (1988). Effects of dithiothreitol, a sulfhydryl reducing agent, on CA_1 pyramidal cells of the guinea pig hippocampus in vitro. *Brain Research* **456**, 49–56.

TWYMAN, R. E., ROGERS, C. J. & MACDONALD, R. L. (1990). Intraburst kinetic properties of the $GABA_A$ receptor main conductance state of mouse spinal cord neurones in culture. *Journal of Physiology* **423**, 193–219.

YOUNG, A. B. & SNYDER, S. H. (1974*a*). Strychnine binding in rat spinal cord membranes associated with the synaptic glycine receptor: cooperativity of glycine interactions. *Molecular Pharmacology* **10**, 790–809.

YOUNG, A. B. & SNYDER, S. H. (1974*b*). The glycine synaptic receptor: evidence that strychnine binding is associated with the ionic conductance mechanism. *Proceedings of the National Academy of Sciences of the USA* **71**, 4002–4005.

WERMAN, R., DAVIDOFF, R. A. & APRISON, M. H. (1967). Inhibition of motoneurones by iontophoresis of glycine. *Nature* **214**, 681–683.